SOLUTION OF THE EULER EQUATIONS IN THE THREE-DIMENSIONAL SPACE USING THE MACCORMACK ALGORITHM - PART I

Edisson Sávio de Góes Maciel
Rua Demócrito Cavalcanti, 152 - Afogados
Recife – PE – Brazil - CEP 50750-080
e-mail: edissonsavio@yahoo.com.br

Abstract. *The present work studies the MacCormack algorithm applied to the solution of the Euler equations in three-dimensional space, solving aerospace problems. A finite volume formulation is used, as also a cell centered data structure and structured spatial discretization of the flow equations. The scheme is second order accurate in space and time. The time integration uses a predictor-corrector scheme with a forward spatial discretization in the predictor step and a backward spatial discretization in the corrector step. An artificial dissipation operator based on the Azevedo work is implemented to guarantee scheme numerical stability in the presence of shock waves and background instabilities. A spatially variable time step is implemented to accelerate the convergence process to the steady state solution. The physical problems of the supersonic flow along a ramp and of the "cold gas" hypersonic flow along a diffuser are studied. In the ramp problem the shock wave is well detected and in the diffuser problem the shock interference is well solved. A final analysis of the computational performance (cost, maximum CFL number and iterations to convergence) is accomplished. The importance of this work is to describe numerical tools that can be used to solve the steady state flowfield of physical problems of interest in the aeronautical and aerospace industry. In this work, the MacCormack algorithm is presented and some results are presented that can be used as reference results to the CFD community.*

Keywords*: MacCormack algorithm, Euler equations, Finite volumes, Three-dimensional space, Supersonic and hypersonic flows.*

1. Introduction

It is necessary to solve the Navier-Stokes equations in the three-dimensional space using turbulence models more precise to obtain more realistic flow properties, inside a reasonable cost interval. Direct simulations or large eddy simulation are still very expensive and require a high computational power which is still elevated to Brazil. Three-dimensional studies start with inviscid simulations, aiming to check the solver to typical problems, and, posteriorly, are intensified to the solution of the laminar Navier-Stokes equations and finally to the turbulent Navier-Stokes equations.

Pulliam and Steger (1980) performed studies with the Navier-Stokes equations, in its thin layer formulation, applied to three-dimensional flows. An implicit finite difference scheme was used to simulations of unsteady flows in configurations of arbitrary geometry through the use of a generalized coordinate system. An implicit approximated factorization technique was employed aiming to obtain better stability conditions in the solution of the viscous flows. The authors emphasized that the implemented scheme could be used to inviscid and viscous, unsteady and steady flows.

Long, Khan and Sharp (1991) developed a method to the solution of the Euler and the Navier-Stokes equations in the three-dimensional space. The method was developed in a finite volume formulation and the spatial discretization could be structured or unstructured to hexahedral or tetrahedral meshes, respectively. It was used a cell centered data structure and the time integration was performed by a Runge-Kutta method of three, four or five stages. The scheme could be symmetrical, with an artificial dissipation operator to guarantee numerical stability, or upwind. In the upwind case, it was used the Roe (1981) scheme. Tests were accomplished with Delta and Lockheed/AFOSR wings.

As can be seen by these two references, three-dimensional algorithms are the objective of any CFD researcher due to its more realistic description of the flowfield of physical problems of interest. As in the Long, Khan and Sharp (1991) work, which used a Jameson and Mavriplis (1986) algorithm version to perform their simulations, the studies with CFD in three-dimensions should start with an algorithm of simple numerical implementation. The Euler equations, as explained above, should be initially considered to simulate flowfield of interest. So, the MacCormack (1969) algorithm is a good choose to perform inviscid numerical experiments in the three-dimensional space due to its simplicity, good solution quality and moderate cost.

In the present work, the MacCormack (1969) scheme is implemented, on the context of finite volumes and using a structured spatial discretization, to solve the Euler equations in the three-dimensional space applied to the problems of the supersonic flow along a ramp and of the "cold gas" hypersonic flow along a diffuser. The implemented scheme is second order accurate in both space and time. It is necessary the introduction of a dissipation operator to guarantee the scheme stability and the Azevedo (1992) model is implemented. The algorithm is accelerated to the steady state solution using a spatially variable time step. The results have demonstrated that the MacCormack (1969) scheme supplies satisfactory solutions, detecting the main flow characteristics, and its cost is comparable to two-dimensional schemes.

Three-dimensional problems are the most realistic situation that can be expected to be simulated and also more complex and the implementation of numerical tools to describe the flowfield of such problems is the objective of any CFD researcher. So, the contribution of the present work is to describe the MacCormack (1969) algorithm in its three-

dimensional version, a popular algorithm in the CFD community due to its numerical simplicity, to solve aeronautical and aerospace problems of interest, a ramp and a diffuser, and present some numerical results that can be used as reference results by the CFD community.

2. Euler equations

The fluid movement is described by the Euler equations, which express the conservation of mass, of momentum and of energy to an inviscid, heat non-conductor and compressible mean, in the absence of external forces. In the integral and conservative forms, these equations can be represented by:

$$\partial/\partial t \int_V Q dV + \int_S \left[E_e n_x + F_e n_y + G_e n_z\right] dS = 0\,, \tag{1}$$

where Q is written to a Cartesian system; V is the cell volume; n_x, n_y and n_z are components of the normal unity vector to the flux face; S is the flux area; and E_e, F_e and G_e are the components of the convective flux vector. The vectors Q, E_e, F_e and G_e are represented by:

$$Q = \begin{Bmatrix} \rho \\ \rho u \\ \rho v \\ \rho w \\ e \end{Bmatrix}, \quad E_e = \begin{Bmatrix} \rho u \\ \rho u^2 + p \\ \rho uv \\ \rho uw \\ (e+p)u \end{Bmatrix}, \quad F_e = \begin{Bmatrix} \rho v \\ \rho uv \\ \rho v^2 + p \\ \rho vw \\ (e+p)v \end{Bmatrix} \quad \text{and} \quad G_e = \begin{Bmatrix} \rho w \\ \rho uw \\ \rho vw \\ \rho w^2 + p \\ (e+p)w \end{Bmatrix}\,, \tag{2}$$

where ρ is the fluid density; u, v and w the Cartesian components of the velocity vector in the x, y and z directions, respectively; e is the total energy per unit volume; and p is the static pressure.

The Euler equations were nondimensionalized in relation to the freestream density, ρ_∞, and the freestream speed of sound, a_∞, for the studied problems. Hence, the density is nondimensionalized in relation to ρ_∞; the velocity components u, v and w are nondimensionalized in relation to a_∞; and the pressure and the total energy are nondimensionalized in relation to the product $\rho_\infty(a_\infty)^2$. The matrix system of Euler equations is closed with the state equation of a perfect gas $p = (\gamma - 1)\left[e - 0.5\rho(u^2 + v^2 + w^2)\right]$, with γ being the ratio of specific heats.

3. MacCormack (1969) algorithm

Using the Green theorem in Equation (1) and adopting a structured mesh notation to the fluid properties and of the flow, it is possible to write that:

$$\partial Q_{i,j,k}/\partial t = -1/V_{i,j,k} \int_{S_{i,j,k}} (\vec{P}\cdot\vec{n})_{i,j,k}\, dS_{i,j,k}\,, \tag{3}$$

with $\vec{P} = \begin{bmatrix} E_e & F_e & G_e \end{bmatrix}^t$, being the convective flux vector. A given computational cell in this notation is formed by the following nodes: *(i,j,k)*, *(i+1,j,k)*, *(i+1,j+1,k)*, *(i,j+1,k)*, *(i,j,k+1)*, *(i+1,j,k+1)*, *(i+1,j+1,k+1)* and *(i,j+1,k+1)*. Details of this representation are available in Maciel (2002) and in Maciel (2004). The calculation of the computational cell volumes is based, in the more general case, on the determination of the volume of one deformed hexahedral in three-dimensional space. This volume is determined by the sum of the volumes of the six tetrahedral which comprise the given hexahedral. The division of the hexahedral in its six tetrahedral components, as well as the vertex nodes which define each cell, can be found in details in Maciel (2002) and in Maciel (2004). In Maciel (2002) is also found details of the calculation of a given tetrahedral volume.

The hexahedral flux area is calculated by the sum of the half areas defined by the norm of the external products $\left|\vec{a}\,x\,\vec{b}\right|$ and $\left|\vec{c}\,x\,\vec{d}\right|$, where $\vec{a}$, $\vec{b}$, $\vec{c}$ and $\vec{d}$ are vectors formed by the nodes which define a given flux surface, as described in Maciel (2002) and in Maciel (2004). The physical quantity $0.5\left(\left|\vec{a}\,x\,\vec{b}\right| + \left|\vec{c}\,x\,\vec{d}\right|\right)$ determines the flux area of each face, which is the area of a deformed rectangle. The normal unity vectors to each flux face are calculated considering the external product $\vec{r}\,x\,\vec{t}\,/\left|\vec{r}\,x\,\vec{t}\right|$ where $\vec{r}$ and $\vec{t}$ are surface crossed vectors (they are the surface diagonals). An additional test is necessary aiming to verify if the normal unity vector is inward or outward of the hexahedral. This test is based on the scalar product $\left[(\vec{r}\,x\,\vec{t}\,)\bullet\vec{f}\,/\left|\vec{r}\,x\,\vec{t}\right|\right]$, where $\vec{f}$ is the vector formed by two nodes: one node refer to the flux face and the other node refer to the immediately opposite face. The positive signal indicates that the vector is inward in the hexahedral. In this case, the vector should be changed by its opposite.

The explicit time march, using the explicit Euler method applied to Eq. (3), leads to the following expression:

$$Q_{i,j,k}^{n+1} = Q_{i,j,k}^{n} - \Delta t / V_{i,j,k} \int_{S_{i,j,k}} (\vec{P} \cdot \vec{n})_{i,j,k} \, dS_{i,j,k} \quad . \tag{4}$$

In the discretization of the surface integral, the Eq. (4) can be rewritten as:

$$Q_{i,j,k}^{n+1} = Q_{i,j,k}^{n} - \Delta t / V_{i,j,k} \left[(\vec{P} \cdot \vec{S})_{i,j-1/2,k} + (\vec{P} \cdot \vec{S})_{i+1/2,j,k} + (\vec{P} \cdot \vec{S})_{i,j+1/2,k} + (\vec{P} \cdot \vec{S})_{i-1/2,j,k} + (\vec{P} \cdot \vec{S})_{i,j,k-1/2} + (\vec{P} \cdot \vec{S})_{i,j,k+1/2} \right]^{n} , \tag{5}$$

where, for example, $\vec{S}_{i,j-1/2,k}$ has the direction and the orientation of the $\vec{n}_{i,j-1/2,k}$ and magnitude equals to the area value $S_{i,j-1/2,k}$. The half indexes indicate fluxes calculated in the respective faces or cell surfaces. Discretizing space and time together, following a Lax-Wendroff type method, dividing the resultant algorithm in two integration time steps (one predictor and the other corrector) and adopting a forward spatial discretization to the predictor step and a backward spatial discretization to the corrector step, it is possible to obtain the MacCormack (1969) algorithm, based on a finite volume formulation, as follows bellow:

- Predictor step:

$$\begin{aligned} \Delta Q_{i,j,k}^{n} = -\Delta t / V_{i,j,k} \Big\{ & \left[(E_e) n_{x\,i,j-1/2,k} + (F_e) n_{y\,i,j-1/2,k} + (G_e) n_{z\,i,j-1/2,k} \right]_{i,j,k} S_{i,j-1/2,k} + \\ & \left[(E_e) n_{x\,i+1/2,j,k} + (F_e) n_{y\,i+1/2,j,k} + (G_e) n_{z\,i+1/2,j,k} \right]_{i+1,j,k} S_{i+1/2,j,k} + \\ & \left[(E_e) n_{x\,i,j+1/2,k} + (F_e) n_{y\,i,j+1/2,k} + (G_e) n_{z\,i,j+1/2,k} \right]_{i,j+1,k} S_{i,j+1/2,k} + \\ & \left[(E_e) n_{x\,i-1/2,j,k} + (F_e) n_{y\,i-1/2,j,k} + (G_e) n_{z\,i-1/2,j,k} \right]_{i,j,k} S_{i-1/2,j,k} + \\ & \left[(E_e) n_{x\,i,j,k-1/2} + (F_e) n_{y\,i,j,k-1/2} + (G_e) n_{z\,i,j,k-1/2} \right]_{i,j,k} S_{i,j,k-1/2} + \\ & \left[(E_e) n_{x\,i,j,k+1/2} + (F_e) n_{y\,i,j,k+1/2} + (G_e) n_{z\,i,j,k+1/2} \right]_{i,j,k+1} S_{i,j,k+1/2} \Big\} \quad , \end{aligned} \tag{6}$$

$$Q_{p\,i,j,k}^{n+1} = Q_{i,j,k}^{n} + \Delta Q_{i,j,k}^{n} \quad .$$

- Corrector step:

$$\begin{aligned} \Delta Q_{c\,i,j,k}^{n+1} = -\Delta t / V_{i,j,k} \Big\{ & \left[(E_e) n_{x\,i,j-1/2,k} + (F_e) n_{y\,i,j-1/2,k} + (G_e) n_{z\,i,j-1/2,k} \right]^{p}_{i,j-1,k} S_{i,j-1/2,k} + \\ & \left[(E_e) n_{x\,i+1/2,j,k} + (F_e) n_{y\,i+1/2,j,k} + (G_e) n_{z\,i+1/2,j,k} \right]^{p}_{i,j,k} S_{i+1/2,j,k} + \\ & \left[(E_e) n_{x\,i,j+1/2,k} + (F_e) n_{y\,i,j+1/2,k} + (G_e) n_{z\,i,j+1/2,k} \right]^{p}_{i,j,k} S_{i,j+1/2,k} + \\ & \left[(E_e) n_{x\,i-1/2,j,k} + (F_e) n_{y\,i-1/2,j,k} + (G_e) n_{z\,i-1/2,j,k} \right]^{p}_{i-1,j,k} S_{i-1/2,j,k} + \\ & \left[(E_e) n_{x\,i,j,k-1/2} + (F_e) n_{y\,i,j,k-1/2} + (G_e) n_{z\,i,j,k-1/2} \right]^{p}_{i,j,k-1} S_{i,j,k-1/2} + \\ & \left[(E_e) n_{x\,i,j,k+1/2} + (F_e) n_{y\,i,j,k+1/2} + (G_e) n_{z\,i,j,k+1/2} \right]^{p}_{i,j,k} S_{i,j,k+1/2} \Big\} \quad , \end{aligned} \tag{7}$$

$$Q_{i,j,k}^{n+1} = 0.5 \left(Q_{i,j,k}^{n} + Q_{p\,i,j,k}^{n+1} + \Delta Q_{c\,i,j,k}^{n+1} \right) \quad .$$

An artificial dissipation operator of second and fourth differences (Maciel and Azevedo, 1998a) is subtracted from the RHS flux terms in the corrector step aiming to provide numerical stability in the proximities of shock waves and uncoupled solutions.

3.1. Artificial dissipation operator

The artificial dissipation operator implemented in the MacCormack (1969) code to simulate three-dimensional flows follows the structure bellow:

$$D(Q_{i,j,k}) = d^{(2)}(Q_{i,j,k}) - d^{(4)}(Q_{i,j,k}) \ , \tag{8}$$

where:

$$\begin{aligned} d^{(2)}(Q_{i,j,k}) = {} & \varepsilon^{(2)}_{i,j,k,1} \frac{(A_{i,j,k} + A_{i,j-1,k})}{2}(Q_{i,j-1,k} - Q_{i,j,k}) + \varepsilon^{(2)}_{i,j,k,2} \frac{(A_{i,j,k} + A_{i+1,j,k})}{2}(Q_{i+1,j,k} - Q_{i,j,k}) \\ & + \varepsilon^{(2)}_{i,j,k,3} \frac{(A_{i,j,k} + A_{i,j+1,k})}{2}(Q_{i,j+1,k} - Q_{i,j,k}) + \varepsilon^{(2)}_{i,j,k,4} \frac{(A_{i,j,k} + A_{i-1,j,k})}{2}(Q_{i-1,j,k} - Q_{i,j,k}) \\ & + \varepsilon^{(2)}_{i,j,k,5} \frac{(A_{i,j,k} + A_{i,j,k-1})}{2}(Q_{i,j,k-1} - Q_{i,j,k}) + \varepsilon^{(2)}_{i,j,k,6} \frac{(A_{i,j,k} + A_{i,j,k+1})}{2}(Q_{i,j,k+1} - Q_{i,j,k}), \end{aligned} \tag{9}$$

named undivided Laplacian operator, is responsible to the numerical stability in the presence of shock waves;

$$\begin{aligned} d^{(4)}(Q_{i,j,k}) = {} & \varepsilon^{(4)}_{i,j,k,1} \frac{(A_{i,j,k} + A_{i,j-1,k})}{2}(\nabla^2 Q_{i,j-1,k} - \nabla^2 Q_{i,j,k}) + \varepsilon^{(4)}_{i,j,k,2} \frac{(A_{i,j,k} + A_{i+1,j,k})}{2}(\nabla^2 Q_{i+1,j,k} - \nabla^2 Q_{i,j,k}) \\ & + \varepsilon^{(4)}_{i,j,k,3} \frac{(A_{i,j,k} + A_{i,j+1,k})}{2}(\nabla^2 Q_{i,j+1,k} - \nabla^2 Q_{i,j,k}) + \varepsilon^{(4)}_{i,j,k,4} \frac{(A_{i,j,k} + A_{i-1,j,k})}{2}(\nabla^2 Q_{i-1,j,k} - \nabla^2 Q_{i,j,k}) \\ & + \varepsilon^{(4)}_{i,j,k,5} \frac{(A_{i,j,k} + A_{i,j,k-1})}{2}(\nabla^2 Q_{i,j,k-1} - \nabla^2 Q_{i,j,k}) + \varepsilon^{(4)}_{i,j,k,6} \frac{(A_{i,j,k} + A_{i,j,k+1})}{2}(\nabla^2 Q_{i,j,k+1} - \nabla^2 Q_{i,j,k}) \end{aligned} \tag{10}$$

named biharmonic operator, is responsible by the background stability.

The following term $\nabla^2 Q_{i,j,k} = [(Q_{i,j-1,k} - Q_{i,j,k}) + (Q_{i+1,j,k} - Q_{i,j,k}) + (Q_{i,j+1,k} - Q_{i,j,k}) + (Q_{i-1,j,k} - Q_{i,j,k}) + (Q_{i,j,k-1} - Q_{i,j,k}) + (Q_{i,j,k+1} - Q_{i,j,k})]$ is named Laplacian of $Q_{i,j,k}$. In the operator $d^{(4)}$, $\nabla^2 Q_{i,j,k}$ is extrapolated from its real neighbor every time that it represents a special boundary cell, recognized in the literature as "ghost" cell. The ε terms are defined as follows:

$$\begin{aligned} & \varepsilon^{(2)}_{i,j,k,1} = K^{(2)} MAX(\nu_{i,j,k}, \nu_{i,j-1,k}), \ \varepsilon^{(2)}_{i,j,k,2} = K^{(2)} MAX(\nu_{i,j,k}, \nu_{i+1,j,k}), \ \varepsilon^{(2)}_{i,j,k,3} = K^{(2)} MAX(\nu_{i,j,k}, \nu_{i,j+1,k}), \\ & \varepsilon^{(2)}_{i,j,k,4} = K^{(2)} MAX(\nu_{i,j,k}, \nu_{i-1,j,k}), \ \varepsilon^{(2)}_{i,j,k,5} = K^{(2)} MAX(\nu_{i,j,k}, \nu_{i,j,k-1}) \text{ and } \varepsilon^{(2)}_{i,j,k,6} = K^{(2)} MAX(\nu_{i,j,k}, \nu_{i,j,k+1}); \end{aligned} \tag{11}$$

$$\begin{aligned} & \varepsilon^{(4)}_{i,j,k,1} = MAX[0, (K^{(4)} - \varepsilon^{(2)}_{i,j,k,1})], \ \varepsilon^{(4)}_{i,j,k,2} = MAX[0, (K^{(4)} - \varepsilon^{(2)}_{i,j,k,2})], \ \varepsilon^{(4)}_{i,j,k,3} = MAX[0, (K^{(4)} - \varepsilon^{(2)}_{i,j,k,3})], \\ & \varepsilon^{(4)}_{i,j,k,4} = MAX[0, (K^{(4)} - \varepsilon^{(2)}_{i,j,k,4})], \ \varepsilon^{(4)}_{i,j,k,5} = MAX[0, (K^{(4)} - \varepsilon^{(2)}_{i,j,k,5})] \text{ and } \varepsilon^{(4)}_{i,j,k,6} = MAX[0, (K^{(4)} - \varepsilon^{(2)}_{i,j,k,6})], \end{aligned} \tag{12}$$

where:

$$\nu_{i,j,k} = \frac{|p_{i+1,j,k} - p_{i,j,k}| + |p_{i,j+1,k} - p_{i,j,k}| + |p_{i-1,j,k} - p_{i,j,k}| + |p_{i,j,k-1} - p_{i,j,k}| + |p_{i,j-1,k} - p_{i,j,k}| + |p_{i,j,k+1} - p_{i,j,k}|}{p_{i,j-1,k} + p_{i+1,j,k} + p_{i,j+1,k} + p_{i-1,j,k} + p_{i,j,k-1} + p_{i,j,k+1} + 6\,p_{i,j,k}} \tag{13}$$

represents a pressure sensor, responsible by the identification of regions of high gradients. The constants $K^{(2)}$ and $K^{(4)}$ has typical values of 1/4 and 3/256, respectively. Every time that a neighbor represents a ghost cell, it is assumed that, for example, $\nu_{i,j-1,k} = \nu_{i,j,k}$. The $A_{i,j,k}$ coefficient was implemented as proposed by Azevedo (1992) and is defined as:

$$A_{i,j,k} = V_{i,j,k} / \Delta t_{i,j,k} \ . \tag{14}$$

4. Spatially variable time step

The idea of a spatially variable time step consists in keeping constant a CFL number in the calculation domain and to guarantee time steps appropriated to each mesh region during the convergence process. The spatially variable time step can be defined by:

$$\Delta t_{i,j,k} = \frac{CFL(\Delta s)_{i,j,k}}{(|q| + a)_{i,j,k}}, \tag{15}$$

where CFL is the Courant number to method stability; $(\Delta s)_{i,j,k}$ is a characteristic length of information transport; and $(|q| + a)_{i,j,k}$ is the maximum characteristic velocity of information transport, where a is the speed of sound. The characteristic length of information transport, $(\Delta s)_{i,j,k}$, can be determined by:

$$(\Delta s)_{i,j,k} = [MIN(l_{MIN}, C_{MIN})]_{i,j,k} , \tag{16}$$

where l_{MIN} is the minimum side length which forms a computational cell and C_{MIN} is the minimum distance of baricenters among the computational cell and its neighbors. The maximum characteristic velocity of information transport is defined by $(|q| + a)_{i,j,k}$, with $q = \sqrt{u^2 + v^2 + w^2}$.

5. Initial and boundary conditions

5.1. Initial condition

The initial condition adopted to the problems is the freestream flow in all calculation domain (Jameson and Mavriplis, 1986). The vector of conserved variables is expressed as follows:

$$Q_\infty = \left\{ 1 \quad M_\infty \cos\theta \quad M_\infty sen\theta \cos\psi \quad M_\infty sen\theta sen\psi \quad \left[\frac{1}{\gamma(\gamma - 1)} + \frac{M_\infty^2}{2} \right] \right\}^t , \tag{17}$$

where M_∞ represents the freestream Mach number, θ is the flow incidence angle downstream the configuration in study and ψ is the angle in the configuration longitudinal plane.

5.2. Boundary conditions

The different types of implemented boundary conditions are described as follows.

a) Wall - The Euler case requires the flux tangency condition. On the context of finite volumes, this imposition is done considering that the tangent velocity component to the wall of the ghost cell be equal to the tangent velocity component to the wall of the neighbor real cell. At the same time, the normal velocity component to the wall of the ghost cell should be equal to the negative of the normal velocity component to the wall of the neighbor real cell. Batina (1993) suggests that these procedures lead to the following expressions to the velocity components u, v and w of the ghost cells:

$$u_g = (1 - 2n_x n_y)u_{real} + (-2n_x n_y)v_{real} + (-2n_x n_z)w_{real} , \tag{18}$$

$$v_g = (-2n_y n_x)u_{real} + (1 - 2n_y n_y)v_{real} + (-2n_y n_z)w_{real} , \tag{19}$$

$$w_g = (-2n_z n_x)u_{real} + (-2n_z n_y)v_{real} + (1 - 2n_z n_z)w_{real} , \tag{20}$$

where n_x, n_y and n_z are normal unity vector components to the face pointing outward of the neighbor real volume.

The fluid pressure gradient in the direction normal to the wall is equal to zero for the inviscid case. The temperature gradient is equal to zero along all wall, with this last situation according to the physical results, without impose, however, the condition of adiabatic wall. With these two conditions, a zero order extrapolation is performed to the fluid pressure and to the temperature. It is possible to conclude that the fluid density will also be obtained by zero order extrapolation.

b) Far field - In the implementation of the boundary conditions in the mesh limit external region to physical problems of external flow, it is necessary to identify four possible situations: entrance with subsonic flow, entrance with supersonic flow, exit with subsonic flow and exit with supersonic flow. These situations are described bellow.

b.1) Entrance with subsonic flow – Considering the one-dimensional characteristic relation concept in the normal direction of flow penetration, the entrance with subsonic flow presents four characteristic velocities of information propagation which have direction and orientation point inward the calculation domain, which implies that the variables associated with these waves can not be extrapolated (Maciel and Azevedo, 1997, Maciel and Azevedo, 1998b, Maciel, 2002, and Maciel, 2004). It is necessary to specify four conditions to these four information. Jameson and Mavriplis (1986) indicate as appropriated quantities to be specified the freestream density and the freestream Cartesian velocity

components u, v and w. Just the last characteristics, "$(q_n\text{-}a)$", which transports information from inside to outside of the calculation domain, can not be specified and will have to be determined by interior information of the calculation domain. In this work, a zero order extrapolation to the pressure is performed, being the total energy defined by the state equation of a perfect gas.

b.2) Entrance with supersonic flow - All variables are specified in the entrance boundary, adopting freestream values.

b.3) Exit with subsonic flow - Four characteristics which govern the Euler equations proceed from the internal region of the calculation domain. So, the density and the Cartesian velocity components are extrapolated from the interior domain. One condition should be specified to the boundary. In this case, the pressure is fixed in the calculation domain exit, keeping its respective value of freestream flow.

b.4) Exit with supersonic flow - The five characteristics which govern the Euler equations proceed from the internal region of the calculation domain. It is not possible to specify variable values at the exit. The zero order extrapolation is applied to density, Cartesian velocity components and pressure.

c) Entrance and exit – The entrance and exit boundaries are applied to both problems. Boundary conditions which involve flow entrance in the calculation domain had the flow properties fixed with freestream values. Boundary conditions which involve flow exit of the computational domain used simply the zero order extrapolation to the determination of properties in this boundary. This procedure is correct because the entrance flow and the exit flow are no minimal supersonic to both studied examples.

6. Results

Tests were accomplished in an ATHLON-2.6GHz and 64 Mbytes of RAM memory microcomputer. Converged results occurred to 4 orders of reduction in the maximum residual value. The value used to γ was 1.4. The configuration downstream angle and the configuration longitudinal plane angle were set equal to 0.0°.

6.1. Ramp physical problem

The algebraic mesh used in this problem has 61 points in the ξ direction, 60 points in the η direction and 10 points in the ς direction, which is equivalent to 31,860 real volumes and 36,600 nodes to the structured discretization of the calculation domain. It was adopted a freestream Mach number of 5.0 as initial condition to this problem, ramp with 20º of inclination.

The MacCormack (1969) scheme used in this simulation a CFL number of 0.5 and the convergence to steady state solution occurred in 421 iterations. Figures 1, 2 and 3 show density, pressure and Mach number contours obtained by this scheme. The Mach number contours present a pre-shock oscillation at the beginning of the ramp. The density and pressure contours present good behavior, without oscillations.

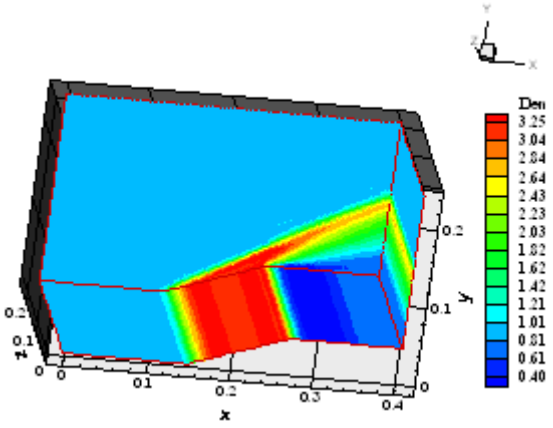

Figure 1 – Density field.

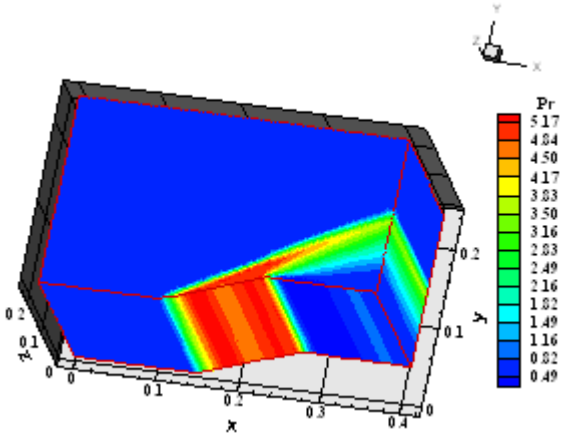

Figure 2 – Pressure field.

Figure 4 show the negative pressure coefficient distribution along the ramp, at section k = kmax/2, where "kmax" represents the maximum number of points in the z direction. The pressure peak reach its maximum value of Cp = 0.38. The expansion fan formed at the ramp end is smooth, appearing a pressure oscillation at its end, which corresponds to the value Cp ≅ -0,05. There are some oscillations in the pressure landing which is typical of second order schemes that can not smooth the pressure peaks originated from discontinuities. In second order TVD schemes, these pressure peaks do not appear because they avoid the appearance of such oscillations in the solution using a modified function (Harten, 1983), for example. The computational cost of the MacCormack (1969) algorithm is 0.0000309s/per volume/per iteration (this cost is the total time of the simulation divided by the number of volumes of the mesh and by the number of iterations to obtain convergence).

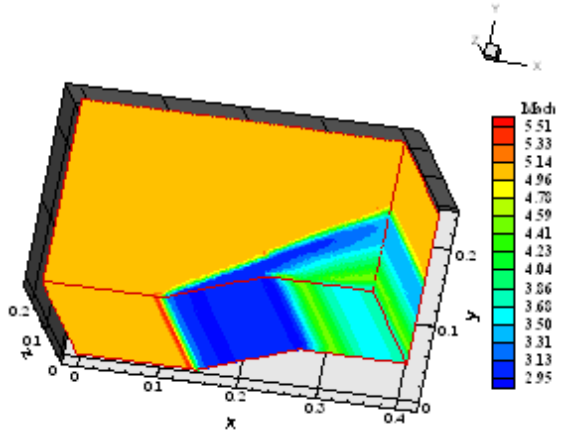

Figure 3. Mach number field.

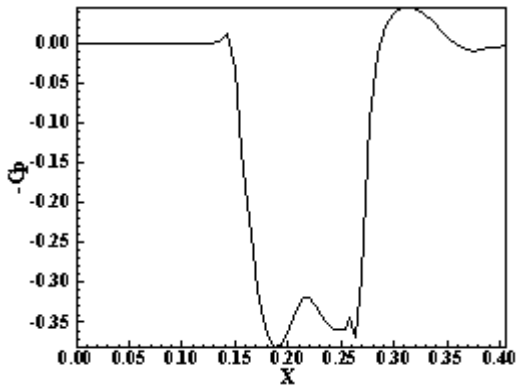

Figure 4. -Cp distribution.

6.2. Diffuser physical problem

The algebraic mesh has 21,600 real volumes and 25,010 nodes to the structured discretization of the calculation domain. It is equivalent to a mesh of 61 points in the ξ direction, 41 points in the η direction and 10 points in the ς direction. The initial condition to the physical problem of the "cold gas" hypersonic flow along a diffuser with 20º of inclination adopted a freestream Mach number of 10.0.

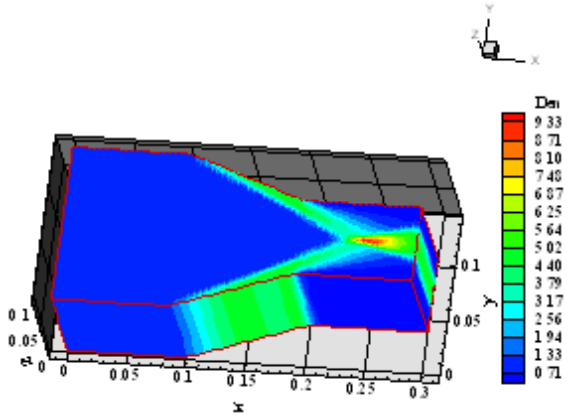

Figure 5. Density field.

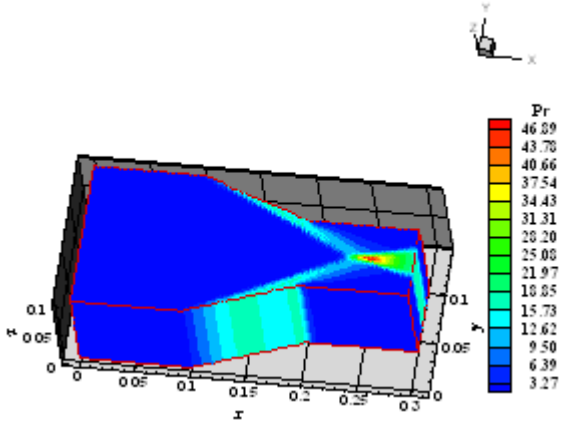

Figure 6. Pressure field.

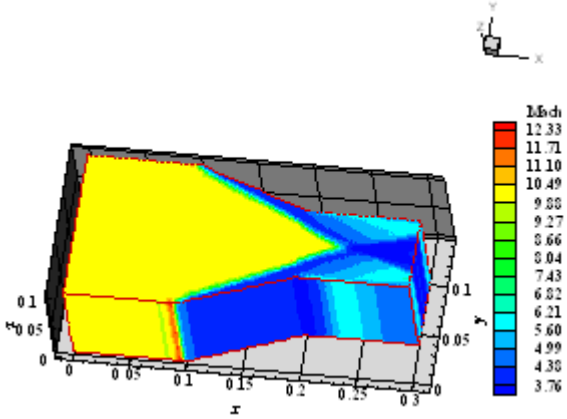

Figure 7. Mach number field.

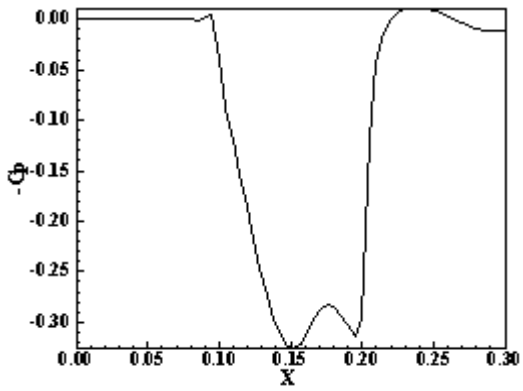

Figure 8. -Cp distribution.

Figures 5, 6 and 7 show the density, pressure and Mach number contours, respectively, obtained by the MacCormack (1969) numerical scheme. Figure 7 show the pre-shock oscillation at the ramp beginning of the diffuser. The density, pressure and Mach number contours present good symmetry and the shock interference between the upper wall shock and the lower wall shock is well highlighted.

Figure 8 shows the –Cp distribution along the diffuser lower wall, to the section k = kmax/2. The peak of Cp at the shock reaches a value of 0.33. The expansion fan in the proximity of the end ramp at the lower wall is smooth,

presenting a reduction in the value of Cp to approximately -0.01. Again, there are some oscillations in the pressure landing which is typical of second order schemes as explained before. The CFL number used in this simulation by the MacCormack (1969) scheme was 0.4 and the convergence occurred in 598 iterations.

7. Conclusions

This work presented the MacCormack (1969) algorithm implemented in its version to three-dimensions. The algorithm is explicit, second order accurate in space and time and integrated in time in two steps: a predictor step, with forward spatial discretization, and a corrector step, with backward spatial discretization. The Euler equations were solved, using a finite volume formulation, with a cell centered data base, and a structured discretization of the flow equations. The physical problems of the supersonic flow along a ramp and of the hypersonic flow along a diffuser were solved. A spatially variable time step was implemented aiming to accelerate the convergence process to steady state condition.

The obtained results were of good quality, occurring just some pre-shock oscillations in the Mach number contours. The density and the pressure fields presented good behavior showing clearly well the shock in the ramp problem and highlighting appropriately the shock interference in the diffuser problem. The -Cp distributions show clearly well the shock and the expansion fan in both problems. Convergences were obtained in less than 600 iterations to both problems. The computational cost of the present MacCormack (1969) algorithm is of 0.0000309s/per volume/per iteration.

8. Acknowledgements

The author thanks the financial support conceded by CNPq under the form of scholarship of process number 304318/2003-5, DCR/1F.

9. References

Azevedo, J. L. F., 1992, “On the Development of Unstructured Grid Finite Volume Solvers for High Speed Flows”, NT-075-ASE-N, IAE, CTA, São José dos Campos, SP.

Batina, J. T., 1993, “Implicit Upwind Solution Algorithms for Three-Dimensional Unstructured Meshes”, AIAA Journal, Vol. 31, No. 5, pp. 801-805.

Harten, A., 1983, “High Resolution Schemes for Hyperbolic Conservation Laws”, Journal Computational Physics, Vol. 49, pp. 357-393.

Jameson, A. and Mavriplis, D., 1986, “Finite Volume Solution of the Two-Dimensional Euler Equations on a Regular Triangular Mesh”, AIAA Journal, Vol. 24, No. 4, pp. 611-618.

Long, L. N, Khan, M. M. S., and Sharp, H. T., 1991, “Massively Parallel Three-Dimensional Euler / Navier-Stokes Method”, AIAA Journal, Vol. 29, No. 3, pp. 657-666.

MacCormack, R. W., 1969, “The Effect of Viscosity in Hypervelocity Impact Cratering”, AIAA Paper 69-354.

Maciel, E. S. G. and Azevedo, J. L. F., 1997, “Comparação entre Vários Algoritmos de Fatoração Aproximada na Solução das Equações de Navier-Stokes”, Proceedings of the 14th Brazilian Congress of Mechanical Engineering (available in CD-ROM), Bauru, SP, Brasil.

Maciel, E. S. G., and Azevedo, J. L. F., 1998a, “Comparação entre Vários Modelos de Dissipação Artificial na Solução das Equações de Navier-Stokes”, Proceedings of the V Congress of Mechanical Engineering North-Northest (V CEM-NNE), Vol. 3, Fortaleza, CE, pp. 604-611.

Maciel, E. S. G. and Azevedo, J. L. F., 1998b, “Comparação entre Vários Esquemas Implícitos de Fatoração Aproximada na Solução das Equações de Navier-Stokes”, RBCM- Journal of the Brazilian Society of Mechanical Sciences, Vol. XX, No. 3, pp. 353-380.

Maciel, E. S. G., 2002, “Simulação Numérica de Escoamentos Supersônicos e Hipersônicos Utilizando Técnicas de Dinâmica dos Fluidos Computacional”, Doctoral thesis, ITA, CTA, São José dos Campos, SP, Brazil, 258 p.

Maciel, E. S. G., 2004, “Relatório ao Conselho Nacional de Pesquisa e Desenvolvimento Tecnológico (CNPq) sobre as Atividades de Pesquisa Desenvolvidas no Primeiro Ano de Vigência da Bolsa de Estudos para Nível DCR-IF Referente ao Processo nº 304318/2003-5”, Technical report to CNPq, November, 37 p.

Pulliam, T. H., and Steger, J. L., 1980, “Implicit Finite-Difference Simulations of three-Dimensional Compressible Flow”, AIAA Journal, Vol. 18, No. 2, pp. 159-166.

Roe, P. L., 1981, “Approximate Riemann Solvers, Parameter Vectors, and Difference Schemes”, Journal of Computational Physics, Vol. 43, pp. 357-372.

10. Responsibility notice

The author is the only responsible for the printed material included in this paper.